*International Journal of Thermophysics, Vol. 10, No. 5, 1989*

# Establishment of an Empirical Correlation for Estimating the Thermal Conductivity of Igneous Rocks[1]

**A. García,[2] E. Contreras,[2] and J. C. Viggiano[3]**

A correlation to predict the thermal conductivity of andesitic igneous rocks is developed from measured data on drill cores from wells from the Los Azufres geothermal field, Mexico. The correlation was developed from density, porosity, and thermal conductivity. Seventeen determinations were made on drill cores extracted at varying depths from 12 wells. Thermal conductivity varied from 1.05 to 2.34 $W \cdot m^{-1} \cdot K^{-1}$, while bulk density varied from 2050 to 2740 $kg \cdot m^{-3}$ and grain density varied from 2610 to 2940 $kg \cdot m^{-3}$. Total porosity varied from 1.9 to 24.7%. Two polynomial regressions, one linear and one quadratic, were tested on the thermal conductivity-times-bulk density product, with total porosity as the independent variable. The correlation coefficients and residual mean square deviations were 0.83 and 0.00491 for the linear fit and 0.87 and 0.00425 for the quadratic model, respectively. For porosities up to about 18%, both models showed very close predictions, but for larger values, the quadratic model appeared to be better and it is recommended for the porosity range from 0 to 25%. Furthermore, density and porosity may be determined from drill cuttings, which are more readily available than cores.

**KEY WORDS:** density; drill cores; geothermal; igneous rocks; thermal conductivity; thermal probe.

## 1. INTRODUCTION

The rocks that form a geothermal reservoir act as structural elements, confining elements, and flow media for the reservoir fluids. Additionally, the

[1] Paper presented at the Tenth Symposium on Thermophysical Properties, June 20–23, 1988, Gaithersburg, Maryland, U.S.A.

[2] Departamento de Geotermia, División Fuentes de Energía, Instituto de Investigaciones Eléctricas, Apartado Postal 475, Cuernavaca, Morelos 62000, México.

[3] Laboratorio de Petrografía, Departamento de Exploración, Gerencia de Proyectos Geotermoeléctricos, CFE, Morelia, Michoacán, México.



0195-928X/89/0900-1063$06.00/0 

rocks act as the principal thermal energy storage medium. The ability with which the rocks can perform these functions determines, to a great extent, the technical and economic feasibility of the resource. Hence, knowledge of the properties and behavior of the reservoir's rocks under *in situ* conditions constitutes a fundamental aspect for evaluation, development, and exploitation of the resource. Yet this aspect has received little attention and becomes a limiting factor of geothermal energy development.

Required properties include porosity, permeability, heat capacity, and thermal conductivity and diffusivity. These properties are normally obtained by core analysis but drill cores are scarce and expensive. If the formation is too fractured, such as in Los Azufres, a core may not even be extracted. Furthermore, thermal conductivity determination is not straightforward and may require large core samples for its measurement. It is thus convenient to have a correlation to predict thermal conductivity from other rock properties which may be easily measured. In this work, a correlation is developed to predict thermal conductivity of igneous rocks from density and porosity measured [1, 2] on drill cores from the Los Azufres field.

A survey of methods to determine thermal conductivity of rocks was summarized in Ref. 3 and correlations to predict thermal conductivity were reviewed in Ref. 4. The survey showed the lack of thermal conductivity data for igneous rocks. The review showed that no correlation to predict thermal conductivity of igneous rocks had been developed, in contrast with a number of available correlations for sedimentary rocks (see Table 1 of Ref. 4). Correlation of thermal conductivity with temperature was presented in Ref. 5 and with pressure in Ref. 6. Rock mineral analyses and conductivity of minerals have been used to estimate thermal conductivity of rocks [6–10]. These methods require specialized equipment to perform the analyses and it may be preferred to measure conductivity directly.

Other correlations include granular materials [11], grain size effects [7], dry and saturated conductivity correlations [12], and inclusion of formation factors [13]. Reddy [14] proposed a simple correlation of conductivity, with density and porosity as independent variables. The present correlation is based on the model of Ref. 14 and is an improvement over the original model of the present authors in two respects: (a) it includes revised data since it was noted in Ref. 4 that some data were physically incongruent, and (b) it includes one extra point which was generated earlier [2].

## 2. EXPERIMENTS

Material selection considered the following aspects.

(a) Availability. This point is a limiting one. Those samples whose availability was in excess of 30 cm in length were selected.

(b) Rock type. The rock types found in the field are pumicitic tuffs and sands, ryolites, and andesites. The andesites are by far the predominant rock type.

(c) Rock texture. Four textures were present in the cores: microcrystalline, microlitic, porfidic, and basaltic. An equal number of samples of each type was included.

(d) Hydrothermal alteration. It is associated with changes in the physical properties of the rocks. Samples covering the widest possible range of alteration were selected.

The samples were petrographically characterized. The analyses were made using point count on thin sections and the number of sections analyzed in each sample varied according to the degree of heterogeneity of each sample.

### 2.1. Bulk Density

Bulk density was measured using recommended techniques [15]. For regularly shaped specimens, volume was measured with a caliper. Mass was determined by weighing a dried sample at 105°C, then exposing it to a pressure of 800 Pa for 1 h and weighing it again. For irregularly shaped specimens, bulk volume was measured by mercury displacement in a porometer. Mass was measured using an electronic precision balance, with a resolution of 0.01 g. The determinations are accurate to within $\pm 10\ \mathrm{kg \cdot m^{-3}}$.

### 2.2. Total Porosity and Solid Density

Total porosity, $\phi_t$, was computed from its definition,

$$\phi_t = 1 - \left(\frac{\rho_b}{\rho_s}\right) \tag{1}$$

where $\rho_b$ is the bulk density and $\rho_s$ is the solid density, which was determined by the pulverization method with 150-$\mu$m-size powder, i.e., displacing an equivalent volume of a liquid which is inert to the solid. Liquid density changes were minimized by using a water bath. Density was also determined using the ASTM Norm C-188-44. In this case, a vacuum

in the liquid–powder suspension was created so that boiling occurred and a vigorous stirring brought the solid into intimate contact with the liquid. The results of both determinations were very similar to those of Ref. 4 and are accurate to within $\pm 30\ \mathrm{kg \cdot m^{-3}}$.

### 2.3. Thermal Conductivity

A transient method [7] was used for thermal conductivity determination. It is based on the relation between the thermal conductivity and the temperature rise of an infinite homogeneous medium caused by a line source of heat of constant strength. The system is governed by

$$\frac{\partial T}{\partial t} = \alpha \left[ \frac{\partial^2 T}{\partial r^2} + \left( \frac{1}{r} \right) \frac{\partial T}{\partial r} \right] \tag{2}$$

where $T$ is temperature, $t$ is time, $\alpha$ is thermal diffusivity ($k/\rho C_p$), $k$ is thermal conductivity, $C_p$ is specific heat, $\rho$ is density, and $r$ is radial distance from the source.

The solution of Eq. (2) for a medium with uniform initial temperature and a heat input $Q$ per unit length of heater is

$$T(r, t) = -\left( \frac{Q}{4\pi k} \right) Ei\left( \frac{-r^2}{4\alpha t} \right) \tag{3}$$

where

$$-Ei(-x) = \int_x^\infty \left( \frac{e^{-u}}{u} \right) du \tag{4}$$

is the exponential integral.

For small values of $x$,

$$Ei(-x) = \gamma + \ln x - x + \frac{x^2}{4} + \mathrm{HOT} \tag{5}$$

where $\gamma = 0.5772...$ is Euler's constant and HOT are higher-order terms. Thus, for large $t$ values,

$$T(r, t) = \left( \frac{Q}{4\pi k} \right) \left[ \ln \left( \frac{4\alpha t}{r^2} \right) - \gamma \right] \tag{6}$$

The temperature rise between $t_1$ and $t_2$ is

$$\Delta T = \left( \frac{Q}{4\pi k} \right) \ln \left( \frac{t_2}{t_1} \right) \tag{7}$$

Thus, the temperature rise versus the log of the time curve approaches a straight line after some time and thermal conductivity is computed from the slope of the straight portion of the curve and the power input.

Figure 1 shows the experimental setup: an electric nickel–chromium heater, 3.2 mm in diameter, is placed along a longitudinal borehole 4.8 mm in diameter in the sample. The sample is an oven-dried cylinder 50.8 mm in diameter and 101.6 mm in length. A type-K thermocouple is attached to the heater at midlength. Another thermocouple is used to monitor the outside surface temperature. Contact resistance is minimized by filling any spaces between the heater and the sample with copper powder. End heat losses were minimized with ceramic insulators. The length-to-diameter ratio of the heat source is within the limits of the recommended theory [16]. When thermal equilibrium was reached, carefully controlled power was applied using a DC power supply. Voltage and current readings were made with a digital multimeter. The applied power created a uniform heat generation along the heater. Data were acquired, recorded, and reduced with a computer system. Thermal conductivity was computed from the slope of a best-fit straight line of the curve of temperature rise versus the logarithm of time. Estimated errors in these determinations amount to $\pm 5\%$. For *in situ* conditions, the sample can be located inside a pressure vessel in the Geothermal Test System shown in Fig. 1.

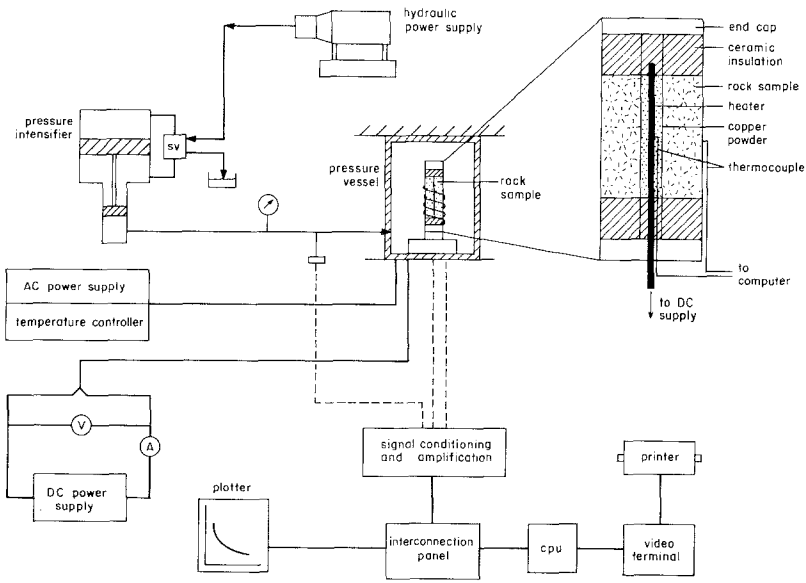


**Fig. 1.** Experimental system for thermal conductivity measurement.

**Table I.** Primary and Hydrothermal Mineral Analyses of Drill Cores[a]

| Well & core | Primary minerals (%) | | | | | Hydrothermal minerals (%) | | | | | | | | | Classification |
|---|---|---|---|---|---|---|---|---|---|---|---|---|---|---|---|
| | PL | CPX | MT | V | ACC | CL | CA | MA | Q | EP | PY | BT | H | AT | |
| Az03(1)a | 28.4 | — | — | — | — | 2.6 | 4.8 | 31.4 | 14.4 | 6.0 | — | — | 12.4 | 59.2 | Andesite |
| Az03(1)b | 24.0 | — | — | — | — | 5.4 | 6.6 | 27.2 | 19.2 | 5.6 | — | — | 12.0 | 64.0 | |
| Az03(1)c | 23.0 | — | — | — | — | 15.4 | 4.6 | 15.0 | 18.8 | 5.0 | — | — | 18.2 | 58.8 | |
| Az03(4)a | 28.4 | 19.6 | — | — | — | 7.2 | — | — | 6.2 | 36.2 | — | — | 2.4 | 49.6 | Basalt |
| Az03(4)b | 25.0 | 13.2 | 0.2 | — | — | 10.0 | — | — | 11.8 | 38.0 | — | — | 1.8 | 59.8 | |
| Az03(4)c | 24.0 | 28.0 | — | — | — | 7.2 | — | — | 9.2 | 31.2 | — | — | 0.4 | 47.6 | |
| Az03(4)d | 29.0 | 19.2 | — | — | — | 7.0 | — | — | 9.8 | 33.6 | — | — | 1.4 | 51.8 | |
| Az03(4)e | 27.4 | 10.0 | — | — | — | 11.6 | — | — | 16.0 | 32.4 | — | — | 2.6 | 60.0 | |
| Az03(4)f | 19.0 | 13.2 | — | — | — | 7.0 | — | — | 17.0 | 43.2 | — | — | 0.6 | 67.8 | |
| Az03(5)a | 61.0 | 11.2 | 7.8 | — | — | 6.6 | — | — | 2.8 | 8.2 | — | — | 2.4 | 17.6 | Basaltic andesite |
| Az03(5)b | 56.4 | 16.4 | 8.2 | — | — | 8.4 | — | — | 1.6 | 9.0 | — | — | — | 19.0 | |
| Az04(3)a | 28.4 | — | — | — | 1.4 | 3.0 | — | 23.4 | 4.8 | 10.2 | — | — | 28.8 | 41.4 | Andesite |
| Az04(3)b | 19.2 | — | — | — | 7.4 | 2.4 | — | 29.6 | 15.6 | 10.6 | — | — | 15.2 | 58.2 | |
| Az04(3)c | 15.2 | — | — | — | 2.8 | 8.6 | — | 13.2 | 16.0 | 14.2 | — | — | 30.0 | 52.0 | |
| Az04(3)d | 15.2 | — | — | — | 7.2 | 7.0 | 6.4 | 27.2 | 24.2 | 12.8 | — | — | — | 77.6 | |
| Az05(1)a | 18.3 | — | — | 24.4 | — | 10.6 | 2.6 | — | — | 6.0 | — | — | 37.6 | 19.2 | Andesite |
| Az05(1)b | 9.0 | — | — | 7.8 | — | 11.8 | 1.0 | — | — | 3.6 | — | — | 66.8 | 16.4 | |
| Az05(1)c | 23.6 | — | — | 8.0 | — | 7.0 | 5.0 | 37.6 | 9.2 | 1.4 | — | — | 8.2 | 60.2 | |
| Az05(1)d | 18.0 | — | — | 9.0 | — | 2.8 | 2.4 | 30.0 | 4.8 | 3.2 | — | — | 29.8 | 43.2 | |
| Az08(2)a | 1.6 | — | — | — | 3.8 | 20.6 | 62.4 | — | 11.0 | — | 0.4 | — | 0.2 | 94.4 | Andesite |
| Az08(2)b | 4.0 | — | — | — | 1.2 | 14.2 | 67.0 | 0.8 | 11.8 | — | 1.0 | — | — | 94.8 | |
| Az08(2)c | 1.4 | — | — | — | — | 13.8 | 45.8 | 2.6 | 19.0 | — | 0.8 | — | 16.6 | 82.0 | |
| Az08(2)d | 1.0 | — | — | — | 0.4 | 13.6 | 25.8 | 3.2 | 54.2 | 0.2 | 1.4 | — | 0.2 | 98.4 | |
| Az08(2)e | 1.6 | — | — | — | 3.2 | 15.8 | 28.6 | 18.6 | 30.8 | 0.2 | 0.6 | — | 0.6 | 94.6 | |

| | | | | | | | | | | | | | | | |
|---|---|---|---|---|---|---|---|---|---|---|---|---|---|---|---|
| Az20(1)a | 6.6 | 0.6 | — | — | 57.2 | 2.8 | 3.0 | 6.6 | 11.8 | — | — | — | 11.4 | 24.2 | Ignimbrite- |
| Az20(1)b | 4.0 | 0.6 | — | — | 35.2 | 1.4 | 0.4 | 4.0 | 6.6 | 0.8 | — | — | 47.0 | 13.2 | (welded tuff) |
| Az20(1)c | 7.2 | — | — | — | 57.2 | 2.6 | 1.0 | 7.6 | 9.8 | 0.4 | — | — | 14.2 | 21.4 | |
| Az20(1)d | 6.2 | 0.2 | — | — | 43.6 | 1.8 | 2.2 | 11.2 | 17.4 | — | — | — | 17.4 | 32.6 | |
| Az20(1)e | 13.2 | 0.6 | — | — | 47.2 | 0.4 | 5.4 | 8.4 | 10.4 | 1.6 | — | — | 12.8 | 26.6 | |
| Az20(3)a | 57.4 | 17.4 | 5.0 | — | — | 10.6 | — | — | — | — | — | — | 9.6 | 10.6 | Basaltic andesite |
| Az20(3)b | 53.6 | 21.6 | 4.6 | — | — | 10.6 | — | — | — | — | — | — | 9.6 | 10.6 | |
| Az22(2)a | 4.8 | — | — | — | — | 16.0 | 9.4 | 15.6 | 44.0 | 2.6 | — | — | 7.6 | 87.6 | Andesite |
| Az22(2)b | 6.4 | — | — | — | — | 12.6 | 6.8 | 13.2 | 27.6 | 3.6 | — | — | 29.8 | 63.8 | |
| Az22(2)c | 16.6 | — | — | — | — | 14.0 | 8.8 | 28.2 | 23.8 | 4.0 | — | — | 4.6 | 78.8 | |
| Az25(1)a | 12.0 | — | — | — | 22.0 | — | 17.8 | 15.0 | 16.8 | — | — | — | 16.4 | 49.6 | Andesite |
| Az25(1)b | 9.0 | — | — | — | 27.0 | — | 8.0 | 34.4 | 19.8 | — | — | — | 1.8 | 62.2 | |
| Az25(1)c | 2.6 | — | — | — | 25.6 | — | 10.2 | 30.4 | 29.8 | — | — | — | 1.4 | 70.4 | |
| Az26(2) | 17.4 | — | — | — | — | 6.6 | 11.0 | 21.2 | 41.0 | 2.8 | — | — | — | 82.6 | Andesite |
| Az26(3)a | 30.0 | — | — | — | 22.2 | 16.2 | 7.8 | — | — | 1.0 | — | — | 22.8 | 25.0 | Basaltic andesite |
| Az26(3)b | 33.8 | — | — | — | 26.0 | 11.8 | 15.4 | — | — | — | — | — | 13.0 | 27.2 | Basaltic andesite |
| Az26(3)c | 32.2 | — | — | — | 29.6 | 11.4 | 20.0 | — | — | — | — | — | 6.8 | 31.4 | Andesite |
| Az29(1)a | 20.4 | — | — | 20.4 | — | — | 9.4 | 15.0 | — | — | — | — | 34.8 | 24.4 | Andesite |
| Az29(1)b | 1.8 | — | — | 3.8 | — | — | 2.4 | 15.2 | — | — | — | — | 76.8 | 17.6 | |
| Az29(1)c | 25.2 | — | — | 25.2 | — | 0.8 | 13.2 | 20.6 | — | — | — | — | 15.0 | 59.8 | |
| Az47(4)a | 50.6 | — | — | — | — | — | — | — | 8.2 | 6.0 | 0.6 | 31.0 | 3.6 | 45.8 | Andesite |
| Az47(4)b | 53.0 | — | — | — | — | — | — | — | 10.0 | 6.6 | 0.6 | 24.6 | 5.2 | 42.0 | |
| Az50(3)a | 67.0 | 1.0 | 7.3 | — | — | 6.4 | — | — | 15.6 | 1.4 | — | — | 10.3 | 23.4 | Lithic tuff |
| Az50(3)b | 33.8 | 4.6 | 5.2 | — | — | 7.4 | 1.6 | — | 18.4 | 0.2 | — | — | 28.8 | 27.6 | |
| Az50(3)c | 25.0 | 1.8 | 9.4 | — | — | 20.4 | 0.4 | — | 16.8 | 3.6 | — | — | 22.6 | 41.2 | |
| Az50(3)d | 36.2 | 4.0 | 6.2 | — | — | 16.4 | — | — | 16.4 | 3.2 | — | — | 17.6 | 36.0 | |
| Az50(3)e | 33.4 | 10.8 | 9.4 | — | — | 11.2 | — | — | 3.3 | 6.6 | — | — | 20.2 | 26.6 | |

[a] ACC, accessories; BT, biotite; CA, calcite; CL, chlorite; CPX, clinopyroxene; EP, epidote; H, voids; MA, clays; MT, magnetite; PL, plagioclase; PY, pyrite; Q, quartz; TA, total alteration; V, glasses.

## 3. RESULTS AND DISCUSSION

### 3.1. Petrographic Analysis

The petrographic analyses showed that all but three samples were andesites, corroborating the abundance of these rocks in the field. The results are shown in Table I. A larger number of analyses was performed on the most heterogeneous rocks. Heterogeneity is the ratio of the standard deviation to the mean value of a given property. The heterogeneity was assigned in six intervals, with the least heterogeneous rocks being analyzed only once, and so on, and a total of 52 analyses was performed. The results of primary and hydrothermal alteration minerals are also shown in Table I. The list is arranged in ascending order of well number.

Of the primary minerals, plagioclase remained unaltered in relatively large amounts, followed by clinopyroxene. Among the hydrothermal minerals, calcite is present in most samples but it is hardly found in the cores from well 3. The core from well 47 is the only one that contains biotite, whereas the core from well 8 has the largest degree of hydrothermal alteration but a relatively low amount of voids. The core from well 26 is highly altered also but has no voids.

**Table II.** Experimentally Determined Density, Porosity, and Thermal Conductivity of Cores from Los Azufres Geothermal Field

| Well and core | Depth (m) | Density ($kg \cdot m^{-3}$) | | Total porosity (%) | Thermal conductivity ($W \cdot m^{-1} \cdot K^{-1}$) |
|---|---|---|---|---|---|
| | | Solids | Bulk | | |
| 3–1 | 600 | 2764 | 2336 | 15.5 | 1.68 |
| 3–4 | 1874 | 2942 | 2555 | 13.2 | 1.84 |
| 3–5 | 2117 | 2804 | 2741 | 2.2 | 1.99 |
| 4–3 | 1000 | 2790 | 2436 | 12.7 | 1.58 |
| 4–3 | 1000 | 2790 | 2431 | 12.9 | 1.53 |
| 5–1 | 600 | 2731 | 2053 | 24.7 | 1.17 |
| 8–2 | 800 | 2789 | 2597 | 6.9 | 2.34 |
| 19–1 | 1000 | 2699 | 2290 | 15.1 | 1.97 |
| 20–1 | 650 | 2606 | 2266 | 13.0 | 1.58 |
| 20–3 | 1600 | 2812 | 2693 | 4.2 | 1.71 |
| 22–2 | 800 | 2720 | 2450 | 9.9 | 2.17 |
| 25–1 | 671 | 2727 | 2324 | 14.8 | 1.75 |
| 26–2 | 596 | 2744 | 2609 | 4.9 | 2.20 |
| 26–3 | 1002 | 2701 | 2429 | 10.1 | 1.55 |
| 29–1 | 400 | 2664 | 2049 | 23.1 | 1.05 |
| 47–4 | 2962 | 2789 | 2737 | 1.9 | 1.89 |
| 50–3 | 1133 | 2679 | 2485 | 7.2 | 1.52 |

### 3.2. Density, Porosity, and Thermal Conductivity

The density, porosity, and thermal conductivity results are shown in Table II. The sampling depth is also shown in Table II. It is noted that about 50% of the cores come from shallow depths, less than 1000 m from the wellhead, and about 3% of the cores come from the 1000- to 1100-m depth interval. The rest of the cores come from depths greater than 1600 m: the core from the deepest origin is that from well 47 at 2962 m.

Solid density ranges from 2606 to 2942 $kg \cdot m^{-3}$, with a mean value of 2760 $kg \cdot m^{-3}$. Similarly, bulk density ranges from 2049 to 2760 $kg \cdot m^{-3}$, with a mean value of 2450 $kg \cdot m^{-3}$. Computed total porosity ranges from 1.9 to 24.7%, with a mean value of 11.3%. Thermal conductivity ranges from 1.05 to 2.34 $W \cdot m^{-1} \cdot K^{-1}$, with a mean value of 1.73 $W \cdot m^{-1} \cdot K^{-1}$. For core numbers 3 and 20, the following trend is noted: as depth increases, bulk density increases, total porosity decreases, and thermal conductivity increases. This, however is reversed for the data of the core from well 26.

A new variable $Y = \log(k\rho_b)$ was formed and is plotted in Fig. 2 as function of the total porosity. Also shown are curves from the regression

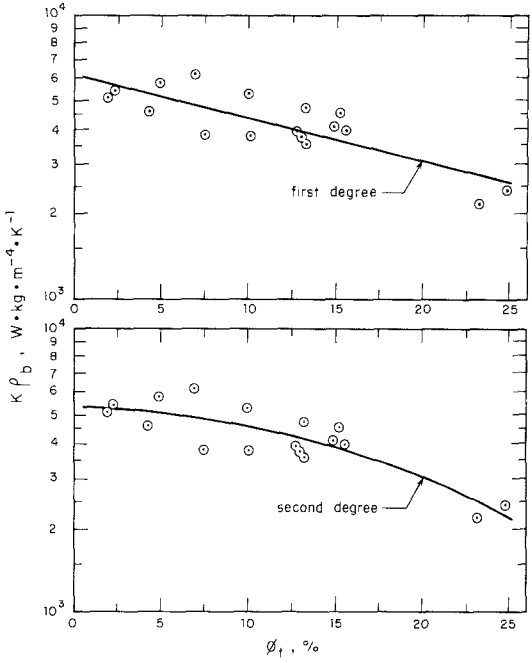


**Fig. 2.** Variation of the product $K\rho_b$ as function of the computed total porosity and polynomials fitted.

analysis described later. Inspection of the figures shows that the data tend to group in the porosity range from 2 to 15% and two points are seen for porosity greater than 20%. Such points correspond to cores from wells 5 and 29. They have the lowest bulk density values, although their solids density is quite close to the mean. Table I shows that both cores have similar primary mineral analyses but their hydrothermal minerals are quite different and their void percentage and hydrothermal alteration are, again, very similar. Since these samples are very porous and have the lowest bulk densities, their thermal conductivity is lowest also.

### 3.3. Correlation Analysis

Two polynomial regressions were performed with total porosity as the independent variable. The inclusion of bulk density and total porosity in the regressions is justified from a heat transfer point of view: they have a direct effect on the physical path for heat flow. Also, these properties are easy to determine and may be obtained from both drill cores and cuttings. The polynomials tested include a linear and a quadratic regression on the $Y$ variable. The resulting curves are shown in Fig. 2. The figure shows that the linear model follows well the data points from about 5 to 15% but deviates at both extremes, while the quadratic model follows all the points better.

Statistical analysis results are shown in Table III. The correlation coefficients are 0.83 and 0.87 for the linear and quadratic models, respectively. The corresponding residual mean square deviations, rms, are $4.91D-3$ and

**Table III.** Statistical Analysis Results for the Correlation

| Variable | Mean value | | SD | Minimum/ maximum | Number of points |
|---|---|---|---|---|---|
| $\phi_t$ | 11.314 | | 6.303 | 1.9/24.7 | 17 |
| $\log(K\rho_b)$ | 3.617 | | 0.118 | 3.332/3.784 | 17 |
| Polynomial degree | Correl. coeff. | rms | Regression coeff. | SE SE | $T$ value |
| 1 | 0.83 | $4.91D-3$ | 3.7931185 | $0.3491D-1$ | 108.64 |
| | dF = 15 | | $-0.155565D-1$ | $0.2696D-2$ | −5.77 |
| 2 | 0.87 | $4.25D-3$ | 3.7221159 | $0.5081D-1$ | 73.26 |
| | dF = 14 | | $-0.472402D-2$ | $0.8667D-2$ | −0.05 |
| | | | $-0.594151D-3$ | $0.3268D-3$ | −1.82 |

$4.25D-3$, respectively. A $D$ is used to indicate that computations were made with double precision. Other data shown are the regression coefficients for each model along with their respective standard errors and $T$-test values. From these data, it is inferred that the quadratic model fits the data best and constitutes the proposed correlation to predict the thermal conductivity of andesitic igneous rocks from the known total porosity and bulk density values. The proposed model, with the $A_i$ given in Table III, is

$$\log_{10}(k\rho_b) = A_0 + A_1\phi_t + A_2\phi_t^2 \tag{8}$$

## 4. CONCLUSIONS

An empirical correlation to predict the thermal conductivity of andesitic igneous rocks from bulk density and total porosity has been developed from experimental data generated from drill cores from the Los Azufres geothermal field, México. The model is a second-order polynomial with porosity as the independent variable and the $Y=\log(k\rho_b)$ product as the dependent variable. The correlation coefficient was 0.87 and the rms was $4.25D-3$. The model is simple in form and easy to use and should be of great value for a number of geothermal activities. Its main advantage is that it is based on easy-to-measure rock properties and may be determined from both drill cores and cuttings.

## REFERENCES

1. E. Iglesias, E. Contreras, and A. García, *Informe IIE/11/2014/I03/F* (Instituto de Investigaciones Eléctricas, Cuernavaca, Mor., México, 1987).
2. E. Contreras, E. Iglesias, and R. Oliver, *Informe IIE/11/3753/I01/F* (Instituto de Investigaciones Eléctricas, Cuernavaca, Mor., México, 1984).
3. A. García and E. Contreras, *Informe IIE/10/11/1663/FE-G29/I07/P* (Instituto de Investigaciones Eléctricas, Cuernavaca, Mor., México, 1985).
4. A. García, E. Contreras, E. Iglesias, and B. Domínguez, *J. Heat Recovery Syst.* **8**:289 (1988).
5. G. Bäckström, in *Proceedings of the Seventh Symposium on Thermophysical Properties* (Am. Soc. Mech. Eng., New York, 1977), pp. 169–180.
6. F. Birch and H. Clark, *Am. J. Sci.* **238**:527 (1940), **238**:613 (1940).
7. W. Woodside and J. H. Messmer, *J. Appl. Phys.* **32**:1688 (1961).
8. A. E. Beck, *The Log Analyst* (1976), p. 30.
9. K. Horai and S. Baldridge, *Earth Planet Inter.* **5**:157 (1972).
10. R. Krupiczka, *Int. Chem. Eng.* **7**:122 (1967).
11. L. F. Martínez, *Proc. First Symp. Cerro Prieto Geothermal Field*, Baja California, México, Report LBL-7098 (Lawrence Berkeley Laboratory, 1978, pp. 342–351.

12. J. Anand, W. H. Somerton, and E. Gomaa, *J. Soc. Pet. Eng.* **13**:267 (1973).
13. H. Zierfuss and G. van der Vliet, *Bull. Am. Assoc. Pet. Geol.* **40**:2475 (1956).
14. M. S. Reddy, in *Proceedings of the Seventh Symposium on Thermophysical Properties* (Am. Soc. Mech. Eng., New York, 1977), pp. 404–411.
15. ISRM, *Commission on Standarization of Laboratory and Field Tests*, International Society for Rock Mechanics, Document No. 2, Lisbon, Portugal (1972).
16. J. H. Blackwell, *Can. J. Phys.* **34**:412 (1956).